A relativistic theory of photoemission from crystalline metals and alloys

1989 J. Phys.: Condens. Matter 1 6483

(http://iopscience.iop.org/0953-8984/1/36/016)

J. Phys.: Condens. Matter 1 (1989) 6483–6501. Printed in the UK

A relativistic theory of photoemission from crystalline metals and alloys

B Ginatempo†, P J Durham‡ and B I Gyorffy§

† Istituto di Fisica Teorica, Facolta' di Scienze, Universita' di Messina, Casella Postale 50, I-98166 Vill. Sant'Agata (Messina), Italy

‡ Daresbury SERC Laboratory, Warrington WA4 DA4, UK

§ H H Wills Physics Laboratory, University of Bristol, Royal Fort, Tyndall Avenue, Bristol BS8 1TL, UK

Received 21 December 1988

Abstract. We develop a theory of energy-, angle- and spin-resolved photoemission spectroscopy of non-magnetic crystalline metals and their alloys on the basis of relativistic quantum mechanics. In particular, the theory is applicable to cases of more than one atom per unit cell and random solid solutions. We illustrate it by explicit first-principles calculations for pure Cu, Ag and Au, ordered Cu_3Au and disordered $Cu_{0.75}Au_{0.25}$.

1. Introduction

The one-electron spectra of crystalline solids play an important role in our understanding of their properties. The only experimental probe that comes close to measuring both the wavevector $\boldsymbol{k}$ and energy E, corresponding to these excitations over a wide range of their values, is angle-resolved photoemission spectroscopy (ARPES). Indeed, difficulties involving the so-called many-body effects and other problems of interpretation notwithstanding, much has been learned about the band structure of solids by this technique (Himpsel 1983, Williams *et al* 1980). In this paper we present a relativistic theory, and its computational implementation, of ARPES. Our aim has been to facilitate the analysis of the very complex data expected, and found, in measurements on metallic alloys containing heavy elements.

While the interpretation of photoemission experiments in terms of the band structure and the notion of direct transitions is often useful (Knapp *et al* 1979), to make the most of the highly structured data it is best, and often necessary, to perform full photocurrent calculations; that is to say, one must consider the transitions from initial states of a semi-infinite solid to the final time-reversed version of the states, usually studied in low-energy electron diffraction (LEED) problems (Mahan 1970, Schaich and Ashcroft 1971, Caroli *et al* 1973). The only formulation of this problem, that is both tractable for first-principles crystal potentials and constitutes a realistic description of the surface is the elegant and very efficient multiple-scattering theory of Pendry (Pendry 1976, Hopkinson *et al* 1980). Most current work, aimed at quantitative calculations of the photocurrent from pure metals, is based on this approach. Moreover, it has been adapted to treating the interesting case of random binary alloys by Durham (1981), who describes the electronic

0953-8984/89/366483 + 19 $02.50

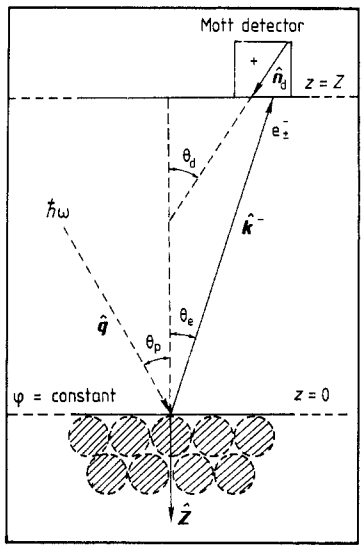

Figure 1. The ideal angle and spin-resolved photoemission experiment and directions and angles definitions.

structure of such alloys within the framework of the first-principles KKR–CPA method (Stocks and Winter 1985, Faulkner 1982) and calculates the configurationally averaged photocurrent (Jordan and Durham 1988). The theory we shall develop in this paper is a relativistic generalisation of those of both Pendry and Durham.

The need to treat the problem at hand relativistically is easily established. As is well known, for the atomic number $Z > 50$ the electronic structure of atoms and solids brims with relativistic effects (Rose 1961). Indeed, it has been studied vigorously in pure metals (McDonald *et al* 1981, Eckardt *et al* 1984), ordered semiconductors (Christensen and Christensen 1986, Fasol *et al* 1988) and random alloys (Staunton *et al* 1983, Ginatempo and Staunton 1988) alike. Moreover, at least in principle, all these calculations have firm foundations in the relativistic spin-density-functional theory (Rajagopal 1978, McDonald and Vosko 1979). Thus calculations that bridge the gap between the first-principles energy bands and the measured photoemission spectra are both needed and timely.

For pure metals the framework for the required calculations of the photocurrent has been already developed. A quite general theory that includes ferromagnetic order on equal footing with relativistic effect was put forward by Ackermann and Feder (1985a). An equivalent formalism for systems without magnetic order was presented by Ginatempo *et al* (1985). Both of these sets of authors have implemented their schemes in physically interesting situations (Ackermann and Feder 1985b, Tamura *et al* 1987, Ginatempo *et al* 1985) and were able to investigate such qualitatively new features of a relativistic treatment as the coupling between the spin and orbital degrees of freedom. Evidently these calculations should be regarded as preliminary forays into a potentially very fertile field of research. A good review of this early work was given by Feder (1985).

All the above calculations follow closely the approach of Pendry. Formally they merely replace the Schrödinger equation for electrons in the presence of incident photons by the corresponding Dirac equation. The part of our work that pertains to pure metals and ordered inter-metallic compounds uses essentially the same formalism. Nevertheless, we recall the basic outline of this theory in § 2, not only as an introduction to our treatment of random alloys in § 3, but also to highlight certain, hitherto unexplored,

aspects of it. In particular, we discuss the exact relativistic version of the acceleration formula for the dipole matrix element (Pendry 1976) and the origin of the relativistic Cooper minima (Kim *et al* 1981). Moreover we study the interesting case of many atoms per unit cell.

In § 3 we present our theory of the configurationally averaged photocurrent from random binary alloys. It is a fairly straightforward relativistic generalisation of the non-relativistic work of Durham (1981).

Finally, we note the ability to calculate on the same footing the photoemission spectra of both ordered inter-metallic compounds and random alloys of the same average composition opens the way to investigations of changes in the electronic structure during an order–disorder transformation (Durham *et al* 1983, Temmerman *et al* 1988). Clearly, such studies are of considerable interest from the point of view of identifying the electronic causes of compositional order (Gyorffy *et al* 1988). We illustrate this feature of the theory by explicit first-principles calculations for the Cu_3Au system. However, we leave the detailed study of the ordering process and comparison of the theory with experiments (Jordan *et al* 1985) to a future publication.

2. A relativistic theory of photoemission from ordered metals

2.1. The multiple-scattering approach to the problem

In figure 1 we give a schematic description of a photoemission experiment. A photon comes in along a given direction $\hat{\boldsymbol{q}} = (\theta_p, \varphi_p)$, and a photoelectron beam is collected in a Mott detector, placed in a plane far from the crystal, along a direction $\hat{\boldsymbol{k}}^- = (\theta_e, \varphi_e)$. The detector internal channels are specified by rotating it to fix a direction $\hat{\boldsymbol{n}}_d = (\theta_d, \varphi_d)$, whose meaning will be clear from the following. We take as the laboratory reference frame a coordinate system having the z axis normal to the surface and oriented towards the bulk crystal.

The motion of an electron is governed by the Dirac Hamiltonian

$$H = c\boldsymbol{\alpha} \cdot [\boldsymbol{p} - (e/c)\boldsymbol{A}(\boldsymbol{r}, t)] + \beta mc^2 + V(\boldsymbol{r}) \tag{1}$$

where c is the speed of the light, e the electronic charge, and m the electronic mass. V is the crystal potential including a surface term. In the Coulomb gauge ($\nabla \cdot \boldsymbol{A} = 0$)

$$\boldsymbol{A}(\boldsymbol{r}, t) = \boldsymbol{a} \exp(\mathrm{i}\boldsymbol{q} \cdot \boldsymbol{r} - \omega t) + \mathrm{HC} \tag{2}$$

with $q = |\boldsymbol{q}| = \omega/c$. The electrostatic potential is

$$V(\boldsymbol{r}) = V_{\mathrm{surf}}(z) + \sum_i{}' V_i(\boldsymbol{r} - \boldsymbol{R}_i) \tag{3}$$

where the sum is limited to the half-space occupied by the atoms at the lattice sites $\boldsymbol{R}_i$. The individual potential wells are centred on the lattice sites and are in the muffin-tin form. The surface barrier is assumed to be step function of height V_0, with respect to the muffin-tin zero. The Dirac matrices α_x, α_y, α_z and β are of the standard form

$$\boldsymbol{\alpha} = \begin{bmatrix} 0 & \boldsymbol{\sigma} \\ \boldsymbol{\sigma} & 0 \end{bmatrix} \qquad \beta = \begin{bmatrix} \mathbf{I} & 0 \\ 0 & -\mathbf{I} \end{bmatrix} \tag{4}$$

where $\boldsymbol{\sigma}$ is the 2×2 Pauli spin-matrix and $\mathbf{I}$ is 2×2 the identity matrix.

In anticipation of using perturbation theory, we may split $\boldsymbol{H}$ into two parts

$$H = H_0 + (\Delta \exp(-i\omega t) + \text{HC}) \tag{5}$$

where

$$H_0 = c\boldsymbol{p} + \beta mc^2 + V(\boldsymbol{r}) \tag{6}$$

and in the electric approximation ($\hbar\omega/mc^2 \ll 1$) the electron–photon vertex is described by

$$\Delta = -e\boldsymbol{\alpha} \cdot \boldsymbol{a} \exp(i\boldsymbol{q} \cdot \boldsymbol{r}) \cong -e\boldsymbol{\alpha} \cdot \boldsymbol{a} \tag{7}$$

In the one-step model of photoemission (Pendry 1976), the rate of probability of finding an electron at the detector, with energy $E + \hbar\omega$ and momentum $\boldsymbol{k}^-$, is

$$I(E, \boldsymbol{k}; \omega, \boldsymbol{q}, \boldsymbol{a}) = \sum_{if} |\langle \Psi_i(E_i)| \Delta |\Psi_f(E_f)\rangle|^2 \, \delta(E_i - E_f + \hbar\omega)$$

$$= \sum_i{}' |\langle \Psi_i(E_i)| \Delta |\Psi_f^{\text{LEED}}(E_i + \hbar\omega)\rangle|^2 = -\frac{\text{Im}}{\pi} \int\int d\boldsymbol{r}\, d\boldsymbol{r}' \Psi_f^{\text{LEED}}$$

$$\times (\boldsymbol{r}; E + \hbar\omega) \Delta G^+(\boldsymbol{r}, \boldsymbol{r}'; E) \Delta^\dagger \Psi_f^{\text{LEED}*}(\boldsymbol{r}'; E + \hbar\omega) \tag{8}$$

where G^+ is the total Green's electronic function for the half-space crystal plus vacuum, and the final state (the so called time reversed LEED state) is

$$\Psi_f^{\text{LEED}}(\boldsymbol{r}; E + \hbar\omega) = \langle \boldsymbol{r}| G^-(E + \hbar\omega)|f\rangle \tag{9}$$

with

$$\langle \boldsymbol{r}|f\rangle = \sum_\lambda q_\lambda U_\lambda(\boldsymbol{k}^-) \exp(i\boldsymbol{k}_\parallel \cdot (\boldsymbol{r} - \boldsymbol{R})_\parallel) \, \delta(z - Z) \tag{10}$$

$$(\boldsymbol{k}^\pm)_\parallel = \boldsymbol{k}; \qquad k_z^\pm = \pm[[2m(E + \hbar\omega - V_0)\{1 + [(E + \hbar\omega - V_0)/mc^2]\}]]^{1/2} \tag{11}$$

where the $\pm$ sign means that the wave is travelling in the positive or negative z direction. Note that $\langle \boldsymbol{r}|f\rangle$ is the plane wave 'at the detector', and the four-spinor amplitude U_λ is defined as

$$U_\lambda^+(\boldsymbol{k}^-) = \left(\frac{E + \hbar\omega - V_0 + 2mc^2}{2(E + \hbar\omega - V_0 + mc^2)}\right)^{1/2} \begin{pmatrix} \chi_\lambda \\ \dfrac{c\boldsymbol{\sigma} \cdot \boldsymbol{k}^-}{E + \hbar\omega - V_0 + 2mc^2} \chi_\lambda \end{pmatrix} \tag{12}$$

where the χ_λ are Pauli spinors. The coefficients q_λ are related to the setting of the Mott detector. These latter quantities will be further specified in the next subsection.

In what follows we exploit the multiple-scattering theory to analyse the quantities appearing in (10), and to work out the necessary expression for calculating the transition-matrix elements, in the dipole approximation, using the solutions of the radial Dirac equations and the muffin-tin potentials.

2.2. The photoelectron beam and its polarisation

The state of an electron in the Mott detector is that of a positive-energy particle moving in a constant potential. Its wavefunction is therefore a Dirac plane wave, to be joined smoothly at the surface to a superposition of Bloch waves propagating throughout the crystal.

The Mott detector measures the spin-polarisation of the photoemitted electrons. The setting of the detector is specified by the coefficients $q_{\lambda=+} = q_+$, $q_{\lambda=-} = q_-$. They are normalised by the requirements

$$|q_+|^2 + |q_-|^2 = 1; \tag{13a}$$

and

$$q_-/q_+ = \exp(i\varphi_d)\tan(\Theta_d/2) \tag{13b}$$

where the angles θ_d and φ_d specify the directions with respect to which the electrons are found to be up and down. In fact, the following cases are distinguished.

(i) The detector can see only 'up' particles then $q_+ = 1, q_- = 0$.
(ii) The detector can see only 'down' particles then $q_+ = 0, q_- = 1$.
(iii) The detector cannot distinguish the λ then $q_+ = 2^{-1/2}, q_- = 2^{-1/2}$.

Note that the Pauli spinors χ_λ in (12) describe polarisation states which are parallel and antiparallel to the direction of $\hat{\boldsymbol{n}}_d$.

The aim of the theory is to calculate

$$I^{\lambda\lambda} = -(\mathrm{Im}/\pi)\langle \Psi^{\mathrm{LEED}}_{f,\lambda} | \Delta G^+(E) \Delta^{\dagger} | \Psi^{\mathrm{LEED}}_{f,\lambda} \rangle \tag{14}$$

starting from

$$\langle r|f,\lambda\rangle = q_\lambda U^+(\boldsymbol{k}^-)\exp(i\boldsymbol{k}_\parallel \cdot (\boldsymbol{r}-\boldsymbol{R})_\parallel)\,\delta(z-Z). \tag{15}$$

The polarisation of the beam will be given by

$$P_z = (I^{++} - I^{--})/I_{\mathrm{tot}} \tag{16}$$

where

$$I_{\mathrm{tot}} = I^{++} + I^{--} \tag{17}$$

is the total photocurrent. The surface parallel components of the polarisation can be measured by changing $\hat{\boldsymbol{n}}_d$. An interesting novel feature of the relativistic photoemission theory is that the beam may be polarised, e.g. $\boldsymbol{P} \neq 0$, even for paramagnetic metals (Ginatempo *et al* 1985, Tamura *et al* 1987).

2.3. *The electric-dipole-matrix elements*

One of the tasks in evaluating the photocurrent given in (14) is the calculation of the dipole-matrix elements. As noted by Pendry (1976), for muffin-tin potentials and a non-relativistic scattering theoretic description of the electrons this is conveniently done by using the acceleration formula

$$\langle E+\hbar\omega|\Delta_{nr}|E\rangle = -(e/mc)\langle E+\hbar\omega|\boldsymbol{p}\cdot\boldsymbol{a}|E\rangle = (ei/mc\omega)\langle E+\hbar\omega|\boldsymbol{a}\cdot\nabla V_i|E\rangle. \tag{18}$$

In this section we derive a relativistic version of this approach.

For the purposes of this discussion it is sufficient to consider the photoemission process for an electron in the field of a single muffin-tin well. Then our aim is to evaluate the relativistic dipole matrix element

$$^t\langle \psi_{\kappa'\mu'}(E+\hbar\omega)| - e\boldsymbol{\alpha}\cdot\boldsymbol{a}|\psi_{\kappa\mu}(E)\rangle \tag{19}$$

where the superscript t means time-reversed, and the four-spinor wavefunctions are (we drop subscripts i and j from the wavefunctions)

$$\psi_{\kappa\mu}(\boldsymbol{r}; E) = \begin{pmatrix} g_\kappa(r; E) & \chi_{\kappa\mu}(\hat{\boldsymbol{r}}) \\ \mathrm{i}f_\kappa(r; E) & \chi_{-\kappa\mu}(\hat{\boldsymbol{r}}) \end{pmatrix} \tag{20}$$

where the upper and lower components g_κ and f_κ are the regular solutions of the coupled first-order differential equations

$$\begin{cases} (E - V_i(r))g_\kappa(r) = c[-\mathrm{d}/\mathrm{d}r + (\kappa - 1)/r]f_\kappa(r) \\ (E - V_i(r) + 2mc^2)f_\kappa(r) = c[\mathrm{d}/\mathrm{d}r + (\kappa + 1)/r]g_\kappa(r) \end{cases} \tag{21}$$

when $r \leqslant R_{\mathrm{mt}}$. For $r > R_{\mathrm{mt}}$ the solution is

$$\psi_{\kappa\mu}(\boldsymbol{r}, E) = -k[\cot \delta_\kappa^i(E) J_{\kappa\mu}(\boldsymbol{r}, E) - N_{\kappa\mu}(\boldsymbol{r}, E)] \tag{22}$$

where the 'Bessel four-spinor' is

$$J_{\kappa\mu}(\boldsymbol{r}, E) = \begin{pmatrix} j_l(kr)\chi_{\kappa\mu}(\hat{\boldsymbol{r}}) \\ \dfrac{\mathrm{i}S_\kappa ck}{E - V_0 + 2mc^2} j_{\bar{l}}(kr)\chi_{-\kappa\mu}(\hat{\boldsymbol{r}}) \end{pmatrix} \tag{23}$$

and the Neumann spinor is the equivalent of (23) but with spherical Neumann functions instead of the Bessel functions j. $\delta_\kappa^i(E)$ is the scattering-phase shift and

$$k = \{2m(E - V_0)[1 + (E - V_0)/mc^2]\}^{1/2}. \tag{24}$$

We introduce the spin-angular harmonics as

$$\chi_{\kappa\mu}(\hat{\boldsymbol{r}}) = \sum_{s=\pm\frac{1}{2}} C_s^{\kappa\mu} Y_{l\mu-s}(\hat{\boldsymbol{r}})\chi_s \tag{25}$$

where χ_s is the Pauli spinor, $Y_{l\mu-s}$ is a complex spherical harmonic, $C_s^{\kappa\mu}$ is a Clebsh–Gordan coefficient and κ is the eigenvalue in the following equation

$$-(\boldsymbol{\sigma} \cdot \boldsymbol{L} + 1)\chi_{\kappa\mu} = \kappa\chi_{\kappa\mu} \tag{26}$$

and is called the spin-angular quantum number. It assumes non-zero integer values and is short for l and j according to the following table

$$\begin{cases} \kappa: & -1 & 1 & -2 & 2 & -3 & 3 & \text{etc.} \\ lj: & s\,\frac{1}{2} & p\,\frac{1}{2} & p\,\frac{3}{2} & d\,\frac{3}{2} & d\,\frac{5}{2} & f\,\frac{5}{2} & \text{etc.} \end{cases}$$

where μ is the azimuthal quantum number ($-j \leqslant \mu \leqslant j$). S_κ is the sign of κ and $\bar{l} = l - S_\kappa$. The time reversal operation applied to the spin angular function produces:

$$\mathrm{TR}\chi_{\kappa\mu} = \chi_{\kappa\mu}^t = -\mathrm{i}\sigma_y\chi_{\kappa\mu}^* = \sum_{s=\pm\frac{1}{2}} (-2s)C_{-s}^{\kappa\mu} Y_{l\mu+s}^*(\hat{\boldsymbol{r}})\chi_s. \tag{27}$$

We are now ready to calculate the dipole matrix element. Substituting (20) in equation (19) we find:

$$\begin{aligned} &{}^t\langle\psi_{\kappa'\mu'}(E + \hbar\omega)| - e\boldsymbol{\alpha} \cdot \boldsymbol{a}|\psi_{\kappa\mu}(E)\rangle \\ &\quad = -e\left[A_{\kappa'\mu'-\kappa\mu}\int r^2\mathrm{d}r\, g_{\kappa'}f_\kappa - A_{-\kappa'\mu'\kappa\mu}\int r^2\mathrm{d}r f_{\kappa'}g_\kappa\right] \end{aligned} \tag{28}$$

where

$$\begin{cases} A_{\kappa'\mu'-\kappa\mu} = \int \mathrm{d}\Omega\, \chi^{\dagger}_{\kappa'\mu'}\boldsymbol{\sigma}\cdot\boldsymbol{a}\chi_{-\kappa\mu} \\ A_{-\kappa'\mu'\kappa\mu} = \int \mathrm{d}\Omega\, \chi^{\dagger}_{-\kappa'\mu'}\boldsymbol{\sigma}\cdot\boldsymbol{a}\chi_{\kappa\mu}. \end{cases} \tag{29}$$

The angular integrals A give rise to the selection rules $\mu + \mu' = 0, \pm 1, \Delta j = 0, \pm 1, \Delta l = \pm 1$. The last two rules might be written in terms of κ as $\kappa' = \kappa \pm S_\kappa, -\kappa$.

The inconvenient feature of (28), the relativistic velocity formula for the dipole matrix element, is that the radial integrals have to be performed for *all* r, not only r within the muffin-tin sphere. In the full theory, where $\psi_{\kappa\mu}$ above is replaced by a Bloch wave, this difficulty is aggravated to the point where, in the interstitial region between the muffin-tin sphere and cell boundary, the angular and the radial integration cannot be separated. Thus considerable computational gain would occur if the matrix elements can be rewritten in such a form that the spatial integration is over the muffin-tin only. This is precisely what the acceleration formula achieves in the non-relativistic discussion of this problem. To find the relativistic analogue of (18) we begin by noting the following identities:

$$\begin{aligned} {}^{t}\langle\psi_{\kappa'\mu'}(E+\hbar\omega)| - e\boldsymbol{\alpha}\cdot\boldsymbol{a}|\psi_{\kappa\mu}(E)\rangle \\ &= -\{e/[2(E+mc^2)+\hbar\omega]\}^{t}\langle\psi_{\kappa'\mu'}(E+\hbar\omega)|[H, \boldsymbol{\alpha}\cdot\boldsymbol{a}]^{+}|\psi_{\kappa\mu}(E)\rangle \\ &= \{2e/[2(E+mc^2)+\hbar\omega]\}^{t}\langle\psi_{\kappa'\mu'}(E+\hbar\omega)|(\boldsymbol{a}\cdot\boldsymbol{p} + V_i\boldsymbol{\alpha}\cdot\boldsymbol{a}/c)|\psi_{\kappa\mu}(E)\rangle \end{aligned} \tag{30}$$

and

$$\begin{aligned} {}^{t}\langle\psi_{\kappa'\mu'}(E+\hbar\omega)|\boldsymbol{a}\cdot\boldsymbol{p}|\psi_{\kappa\mu}(E)\rangle &= (1/\hbar\omega)^{t}\langle\psi_{\kappa'\mu'}(E+\hbar\omega)|[H, \boldsymbol{a}\cdot\boldsymbol{p}]^{-}|\psi_{\kappa\mu}(E)\rangle \\ &= (\mathrm{i}/\omega)^{t}\langle\psi_{\kappa'\mu'}(E+\hbar\omega)|\boldsymbol{a}\cdot\boldsymbol{\nabla}V_i|\psi_{\kappa\mu}(E)\rangle \\ &= (\mathrm{i}/\omega)D^{*}_{\kappa'\mu'\kappa\mu}\int r^2\,\mathrm{d}r\,(\mathrm{d}V_i/\mathrm{d}r)\,(g_{\kappa'}g_\kappa + f_{\kappa'}f_\kappa) \end{aligned} \tag{31}$$

where the symbol $[\,]^{-(+)}$ stands for commutator (anti-commutator), and

$$\begin{aligned} D_{\kappa\mu\kappa'\mu'} &= \int \mathrm{d}\Omega\, \chi^{\dagger}_{\kappa\mu}(\boldsymbol{a}\cdot\hat{\boldsymbol{r}})^{*}\chi_{\kappa'\mu'} = D_{-\kappa\mu-\kappa'\mu'} \\ &= \sum_{s=\pm\frac{1}{2}}(-2s)C^{\kappa\mu}_{s}D^{\mathrm{non}}_{l\mu-s\,l'\mu'+s}C^{\kappa'\mu'}_{-s}. \end{aligned} \tag{32}$$

Here the non-relativistic photoemission angular integrals, D^{non} (see Pendry 1976) are defined by

$$D^{\mathrm{non}}_{l\mu-s\,l'\mu'+s} = (4\pi/3)|\boldsymbol{a}|\sum_{m''=-1}^{1}Y^{*}_{1m''}(\hat{a})\int \mathrm{d}\Omega\, Y^{*}_{l\mu-s}(\Omega)Y_{1m''}(\Omega)Y^{*}_{l'\mu'+s}(\Omega). \tag{33}$$

Exploiting the radial Dirac equations (21) and substituting in the commutation relations (30) and (31), we find a simple arithmetic relation between the coefficients D (equation (32)) and A (equation (29)):

$$\begin{cases} A_{\kappa'\mu'-\kappa\mu} = \mathrm{i}(\kappa - \kappa' - 1)D^{*}_{\kappa'\mu'\kappa\mu} \\ A_{-\kappa'\mu'\kappa\mu} = \mathrm{i}(\kappa' - \kappa - 1)D^{*}_{\kappa'\mu'\kappa\mu}. \end{cases} \tag{34}$$

Finally putting everything together yields the principle result of this section:

$$^{t}\langle\psi_{\kappa'\mu'}(E+\hbar\omega)|-e\boldsymbol{\alpha}\cdot\boldsymbol{a}|\psi_{\kappa\mu}(E)\rangle=\{2iec/[2(E+mc^2)+\hbar\omega]\omega\}\,D^{*}_{\kappa'\mu'\kappa\mu}M_{\kappa\kappa'} \tag{35}$$

$$M_{\kappa\kappa'}=\int r^2\,dr\left(\frac{dV_i}{dr}(g_{\kappa'}g_{\kappa}+f_{\kappa'}f_{\kappa})+\frac{i\omega V_i}{c}[g_{\kappa'}f_{\kappa}(\kappa'-\kappa-1)+f_{\kappa'}g_{\kappa}(\kappa'-\kappa+1)]\right). \tag{36}$$

Evidently our aim to circumvent the spatial integration outside the muffin-tin sphere has been achieved since dV_i/dr and V_i are both zero beyond the muffin-tin radius.

It is reassuring to note that in the $c\rightarrow\infty$ limit (36) reduces to

$$M_{ll'}=\int r^2\,dr\,R_{l'}\frac{dV_i}{dr}R_l \tag{37}$$

where $R_l(r,E)$ are the radial solution of the appropriate Schrödinger equation for the orbital quantum number l and energy E, and which is the usual non-relativistic acceleration formula. Ackermann and Feder (1985a, b) were able, exploiting the Green theorem, to write down another formula that, although the integration is limited to the muffin-tin radius, does not reduce at glance to the non-relativistic counterpart when the $c\rightarrow\infty$ limit is taken.

Before moving on with our theory of photoemission in the next section we shall pause, briefly, to examine some interesting consequences of the dipole-matrix-element formulae in equations (35) and (36).

2.4. The relativistic Cooper minima

In addition to being useful in the numerical evaluation of the dipole matrix elements, equation (36) has a number of attractive features of general significance. One of these is the ease with which it leads to the explanation of the occurrence of minima in the dipole oscillator strength as a function of the incident photon frequency. These are the famous Cooper minima discovered in the non-relativistic quantum mechanics by Cooper (Cooper 1962, Fano and Cooper 1968). In that context it was understood as minima in the square of the radial integrals

$$\int r^2\,dr\,R_l(E)\,r\,R_{l+1}(E+\hbar\omega)=\frac{2}{\omega^2}\int r^2\,dr\,R_l\frac{dV_i}{dr}R_{l+1}$$

due to the 'moving in' towards the origin of the nodes of the high energy wavefunction for increasing photon energy. The minimum in the oscillator strength occurs at an energy where the node in a wavefunction coincides spatially with a maximum in the other.

Subsequently, it was noted that the Cooper minima are also a feature of the relativistic theory and that relativistic effects can dramatically alter their shape and position (Kim *et al* 1981). As was stressed by Fano (1969), relativistic effects are more pronounced for circularly polarised light with frequency near the Cooper minima.

As an illustration, we have calculated the oscillator strength for a single muffin-tin well of Au, for the 'd–f' permitted transitions, starting from an initial energy of $E=0.6$ Ryd. above the muffin-tin zero, as a function of the photon frequency. Figure 2 shows the logarithm of the oscillator strengths for the indicated transitions and one can see that each of the curves has a sharp minimum. These minima correspond to the oscillator strengths zeroes, and occur at $\hbar\omega=205$ eV for the ($\kappa=2$, $\kappa'=3$) transition (the dashed curve in figure 2), at $\hbar\omega=185$ eV for the ($\kappa=-3$, $\kappa'=3$) one (dotted

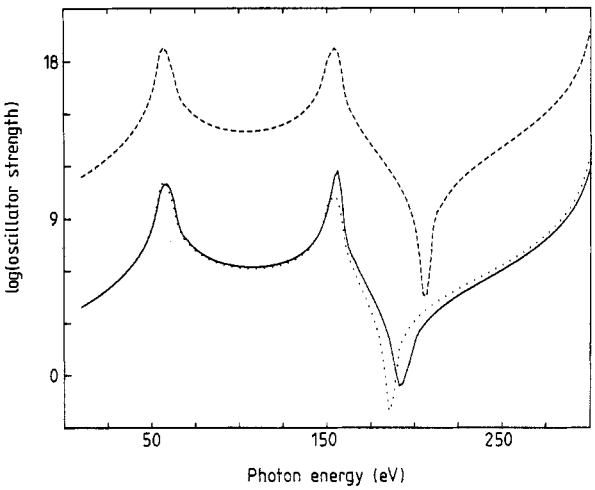

Figure 2. The logarithm of the oscillator strengths for the d–f dipole transitions as a function of the photon frequency. ($l = 2, j = 3/2) \rightarrow (l = 3, j = 5/2)$ transition: broken curve; ($l = 2$, $j = 5/2) \rightarrow (l = 3,\ j = 5/2)$ transition: dotted curve; ($l = 2,\ j = 5/2) \rightarrow (l = 3,\ j = 7/2)$ transition: full curve.

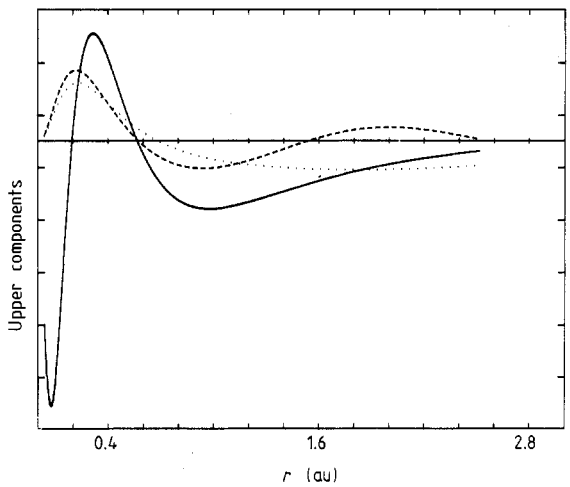

Figure 3. The upper components wavefunctions $g_{\kappa=-3}(r, \varepsilon)$ (full curve), $g_{\kappa=-4}(r, \varepsilon + 50\,\text{eV})$ (dotted curve), and $g_{\kappa=-4}(r, \varepsilon + 200\,\text{eV})$ (broken curve). The muffin-tin radius is $R_{\text{mt}} = 2.511$ au.

curve) and at $\hbar\omega = 190$ eV for the ($\kappa = -3$, $\kappa' = -4$) one (full curve). Figure 3 shows the initial-state large components of the wavefunctions ($0 < r < R_{\text{mt}} = 2.511$ au) for $\kappa = -3$, and the same for two high energies, corresponding to $\hbar\omega = 50$ and 200 eV respectively, and for $\kappa' = -4$. One can see that the high-energy large components are close to each other for $r < 1.0$ au, but for higher radii the 200 eV one bends up and crosses zero, while the other tends to saturate. This circumstance together with the r^2 factor in the integral makes the leading term of the radial integral for the case $\hbar\omega =$ 200 eV rather smaller than the other case due to the new negative contribution. There

must be, therefore a photon frequency at which the oscillator strength vanishes. The presence of the other terms related to the lower components, which are much smaller, eventually produces shifts of the zeroes. We note that this argument for the physical origin of the minima is just that of Cooper (1962), with relativistic corrections.

2.5. The relativistic LEED formulae for photoemission

Equation (15) is a plane wave incident onto the surface of the crystal. To calculate the time reversed LEED state in equation (9) properly we must allow this wave to be scattered by the crystal, i.e. a slab of non-equivalent layers (see for example Pendry 1974, Feder 1981). We now present the formulae for the case of a one-atom-per-layer unit-cell crystal and for a bulk-repeat unit made by one layer.

In the atom placed at the origin c_n of the n-th layer we have an incident wave given by

$$\psi_\lambda^n = \sum_{g,s} W_{gs}^{+0\lambda n} \exp[\mathrm{i}\boldsymbol{K}_g^+ \cdot (\boldsymbol{r} - \boldsymbol{c}_n)] + \sum_{g,s} W_{gs}^{-0\lambda n} \exp[\mathrm{i}\boldsymbol{K}_g^- \cdot (\boldsymbol{r} - \boldsymbol{c}_n)] \tag{38}$$

with

$$(\boldsymbol{K}_g^\pm)_\parallel = (\boldsymbol{k} + \boldsymbol{g})_\parallel$$
$$K_{gz}^\pm = \pm[[2m(E + \hbar\omega - V_0)\{1 + [(E + \hbar\omega - V_0)/mc^2]\} - |\boldsymbol{k} + \boldsymbol{g}|^2]]^{1/2} \tag{39}$$

where $\boldsymbol{g}$ is a layer reciprocal lattice vector. Evidently ψ_λ^n consists of a forward- and a backward-travelling plane wave. The $\boldsymbol{W}$ are spinor amplitudes as for equation (12). Now we expand this plane wave in spherical waves.

$$\psi_\lambda^n = \sum_{\kappa\mu} A_{\kappa\mu}^{0\lambda n} J_{\kappa\mu}^t(r; E + \hbar\omega) \tag{40}$$

with

$$A_{\kappa\mu}^{0\lambda n} = 4\pi \sum_{g,s} \mathrm{i}^l(-2s)(-1)^{\mu - s}[Y_{l-\mu+s}(\hat{K}_g^+)W_{gs}^{+0\lambda n} + Y_{l-\mu+s}(\hat{K}_g^-)W_{gs}^{-0\lambda n}] \tag{41}$$

where the W are the scalar coefficients of the corresponding $\boldsymbol{W}$. Scattering theory allows us to construct the spherical wave amplitude of a wave scattered by a layer as

$$A_{\kappa\mu}^{\lambda n} = \sum_{\kappa'\mu'} A_{\kappa'\mu'}^{0\lambda n} \tau_{\kappa'\mu'\kappa\mu}^n(\boldsymbol{k}_\parallel, E + \hbar\omega) \tag{42}$$

where

$$\tau_{\kappa'\mu'\kappa\mu}^n(\boldsymbol{k}_\parallel, E + \hbar\omega) = ((t^n)^{-1} - G_{\mathrm{lay}}^{0n})_{\kappa'\mu'\kappa\mu}^{-1} \tag{43}$$

τ^n is the scattering path operator for the n-th layer, G_{lay}^0 the relatavistic KKR structure constants for the same layer and t is the single site t-matrix, whose 'on-energy-shell' components are given in terms of the scattering phase shifts as

$$t_\kappa^n = -(1/k) \sin \delta_\kappa^n \exp(\mathrm{i}\delta_\kappa^n). \tag{44}$$

By means of the scattering path operator we can define the transmission coefficient of a

layer, i.e. the plane wave matrix element of τ^n in terms of the forward $(+z)$ travelling waves:

$$T_{gg'}^{n++ss'} = \delta_{gg'ss'} - \frac{8\pi^2 i}{\Omega K_{gz}^+} \sum_{\kappa\kappa'\mu\mu'} [\mathrm{i}^{-l} C_s^{\kappa\mu} Y_{l\mu-s}(\boldsymbol{K}_g^+) \tau_{\kappa\mu\kappa'\mu'}^n(\boldsymbol{k}_\parallel, E + \hbar\omega)$$

$$\times \mathrm{i}^{l'} C_{s'}^{\kappa'\mu'} Y_{l'\mu'-s}^*(\boldsymbol{K}_{g'}^+)] \tag{45}$$

Similarly, the backward–forward matrix element of the τ^n matrix is the reflection matrix of the layer itself:

$$R_{gg'}^{n-+ss'} = -\frac{8\pi^2 i}{\Omega K_{gz}^+} \sum_{\kappa\kappa'\mu\mu'} [\mathrm{i}^{-l} C_s^{\kappa\mu} Y_{l\mu-s}(\boldsymbol{K}_g^+) \tau_{\kappa\mu\kappa'\mu'}^n(\boldsymbol{k}_\parallel, E + \hbar\omega)$$

$$\times \mathrm{i}^{l'} C_{s'}^{\kappa'\mu'} Y_{l'\mu'-s'}^*(\boldsymbol{K}_{g'}^-)]. \tag{46}$$

It is interesting to note the following identities that make this relativistic treatment different from the non-relativistic one (Pendry 1974):

$$R_{gg'}^{-+ss'} = (-1)^{(s-s')} R_{gg'}^{+-ss'} \qquad T_{gg'}^{--ss'} = (-1)^{(s-s')} T_{gg'}^{++ss'}. \tag{47}$$

Equations (42)–(47) solve the multiple scattering problem of an isolated layer. We now have to bring together many layers by shifting their origins, and take into account the multiple-scattering corrections due to the presence of these many layers. To accomplish that there is a number of standard procedures in LEED-type calculations (see for example Feder 1981, and references therein). We use the layer-doubling method (Pendry 1974 and 1976) to calculate the bulk reflectivity and to achieve that we need to add an imaginary part to the energy, so that the plane waves will become evanescent, therefore their amplitudes will fade after a certain penetration depth, limiting so the number of layers entering in the calculation. One ends with an expression similar to equation (38) where the $W^{\pm}$ coefficients this time contain information about multiple scattering. Transforming the related plane waves in spherical waves we end up with:

$$\Psi_\lambda^n = \sum_{\kappa\mu} A_{\kappa\mu}^{\lambda n} \psi_{\kappa\mu}^n(r; E + \hbar\omega). \tag{48}$$

The same calculation can provide the low energy state, with a formula entirely analogous to equation (48), but in which all the quantities are calculated for the energy E and momentum $-\boldsymbol{k}_\parallel + \boldsymbol{q}$. The other fundamental difference is that while the incident wave for the LEED state is just a free-space plane wave at the surface, the incident wave amplitude is the amplitude of probability of the transition from a time reversed LEED state down to the low energy state in the bulk (Pendry 1976, Hopkinson *et al* 1980).

In the case of more complex structures (say $L1_2$, DO_{22}, etc.), the above formulae are easily generalisable. It is enough to consider the label n as representing the couple (m, i) for the m-th layer and for the i-th atom in the m-th layer unit cell, in the formulae (41)–(45), and to consider the repeat bulk unit as made up of many layers in the layer doubling method and in the formulae like equations (38) and (41). The other difference is some phase factor $\exp(\pm \mathrm{i}\boldsymbol{k}_g \cdot \boldsymbol{u}_i)$ where $\boldsymbol{u}_i$ is the position of the i-th atom in the unit cell to be inserted properly in equations (41), (45) and (46).

2.6. The photocurrent formulae

Following Pendry's non-relativistic theory we may break the total photocurrent into four self-explanatory contributions:

$$I^{\lambda\lambda} = I^{\lambda\lambda}_{\text{at}} + I^{\lambda\lambda}_{\text{intra}} + I^{\lambda\lambda}_{\text{inter}} + I^{\lambda\lambda}_{\text{surf}} \tag{49}$$

where

$$I^{\lambda\lambda}_{\text{at}} = -\frac{\text{Im}}{\pi}\sum_n \sum_{\kappa\kappa'\kappa''\mu\mu'\mu''} A^{\lambda n}_{\kappa'\mu'} D^*_{\kappa'\mu',\kappa\mu} t^n_\kappa M^n_{\kappa\kappa'\kappa''} D_{\kappa\mu,\kappa''\mu''} A^{\lambda n *}_{\kappa''\mu''} \tag{50}$$

i.e. the photocurrent produced by an isolated atom where $M^n_{\kappa\kappa'\kappa''}$ is a radial double integral involving the dipole moment operator (cf equation (36)) and the low energy single site Green function defined as

$$G^{00}(r, r'; E) = \sum_{\kappa\mu} \psi_{\kappa\mu}(r, E)\, t^n_\kappa \psi^\dagger_{\kappa\mu}(r', E) - \sum_{\kappa\mu} \zeta_{\kappa\mu}(r_>; E)\psi^\dagger_{\kappa\mu}(r_<; E) \tag{51}$$

where the subscript $>$ stands for the greater magnitude of $\boldsymbol{r}$ or $\boldsymbol{r}'$ and $\zeta_{\kappa\mu}$ is the irregular solution of the Dirac equation that joins smoothly at the muffin-tin radius to $J_{\kappa\mu}$.

The multiple scattering corrections $I^{\lambda\lambda}_{\text{mult}} = I^{\lambda\lambda}_{\text{intra}} + I^{\lambda\lambda}_{\text{inter}}$ may be written as

$$I^{\lambda\lambda}_{\text{mult}} = -\frac{\text{Im}}{\pi}\sum_n \Bigg\{ \sum_{\{\kappa\mu\}} A^{\lambda n}_{\kappa_1\mu_1} D^*_{\kappa_1\mu_1,\kappa_2\mu_2} M^{n(2)}_{\kappa_1\kappa_2} (\tau^n_{\kappa_2\mu_2\kappa_3\mu_3} - t^n_{\kappa_2}) \times M^{n(1)}_{\kappa_3\kappa_4} D_{\kappa_3\mu_3\kappa_4\mu_4} A^{\lambda n *}_{\kappa_4\mu_4} \Bigg\}. \tag{52}$$

Here $M^{n(1)}_{\kappa\kappa'}$ is:

$$M^{n(1)}_{\kappa\kappa'} = \int r^2\, \text{d}r \Bigg\{ \frac{\text{d}V^n}{\text{d}r} (g^{n*}_{\kappa'} g^n_\kappa + f^{*n}_{\kappa'} f^n_\kappa) - \frac{\text{i}\omega V^n}{c} [g^{n*}_{\kappa'} f^n_\kappa(\kappa' - \kappa - 1) + f^{n*}_{\kappa'} g^n_\kappa(\kappa' - \kappa + 1)] \Bigg\} \tag{53}$$

and $M^{n(2)}_{\kappa\kappa'}$ is:

$$M^{n(2)}_{\kappa\kappa'} = \int r^2\, \text{d}r \Bigg\{ \frac{\text{d}V^n}{\text{d}r} (g^n_{\kappa'} g^n_\kappa + f^n_{\kappa'} f^n_\kappa) + \frac{\text{i}\omega V^n}{c} [g^n_{\kappa'} f^n_\kappa(\kappa' - \kappa - 1) + f^n_{\kappa'} g^n_\kappa(\kappa' - \kappa + 1)] \Bigg\} \tag{54}$$

where primed variables refer to the high energy state and complex conjugations take into account properly for time reversal and the fact that, owing to the layer doubling method, the energy E is a complex variable. The τ matrix in equation (52) depends on the energy E and momentum $-\boldsymbol{k}_\parallel + \boldsymbol{q}$. The surface term is:

$$I^{\lambda\lambda}_{\text{surf}} = -\frac{\text{Im}}{\pi}\sum_{g,s} [W^{+\lambda 0}_{-gs} + W^{-\lambda 0}_{-gs}] \frac{\text{i}a_z V_0}{2mc^2} \exp(\text{i}\boldsymbol{q}\cdot\boldsymbol{c}_0)[w^{+\lambda 0}_{gs} + w^{-\lambda 0}_{gs}] \tag{55}$$

i.e. the photocurrent produced by the surface barrier. The w coefficients are the relativistic generalisation of Pendry's (1976).

In passing we note that the presence of the scattering path operator τ^n in equation (52) provides a direct link between the photoemission spectra and the band structure of the crystal owing to the following identities:

$$\tau(\boldsymbol{k}, E) = [t^{-1}(E) - G^0_{\mathrm{KKR}}(\boldsymbol{k}, E)]^{-1} \tag{56}$$

$$\tau(\boldsymbol{k}, E) = \sum_{ij} \tau^{ij}(E) \exp[\mathrm{i}\boldsymbol{k} \cdot (R_i - R_j)]$$

$$= \sum_{nn'}^{\infty} \sum_{ij}{}' \tau^{i(n)j(n')}(E) \exp(\mathrm{i}\boldsymbol{k}_{\parallel} \cdot (\boldsymbol{R}_i^n - \boldsymbol{R}_j^{n'})) = \sum_{n}^{\infty} \tau^n(\boldsymbol{k}_{\parallel}, E) \tag{57}$$

where n runs over the layers and the primed sum is over the lattice positions belonging to the n-th layer. The determinant of the inverse matrix in equation (56) is the so called KKR determinant whose zeroes define the band structure. Equation (56) directly relates photoemission spectra to that. We want also to remark that the above formulae enables us to calculate the 'one-particle' angle-resolved photoemission spectrum, for given surface and photon polarisations. Exchange and correlation effects are 'frozen' as they were in the ground state (this is the case when as input an LDA effective muffin-tin potential is used). However such a calculation makes possible a direct comparison with experimental measurements any time one may neglect 'many-body' effects and secondary electron emission (which is not in this theory either).

As in the former subsection these formulae are applicable to the case of many-atom-per-unit-cell crystals, just visualising the sums over n (Σ_n) as being sums over number of atoms per unit cell and repeat units as well.

2.7. Normal emission from the (1, 1, 1) surface of Cu, Ag and Au

As an illustration of the above theory we performed calculations of the photoemission spectra from the (1, 1, 1) surface of the noble metals. The results are shown in figure 4. The incidence angle is 50°, the emission angle is 0 (normal emission) and the reaction plane is the ΓKWL. The photon frequency is $\omega = 21.2$ eV (HeI), and the calculations were performed for both an s-polarised (the electric field parallel to the surface and orthogonal to the reaction plane) and a p-polarised (the electric field lies in the reaction plane and has a component orthogonal to the surface) photon beam. The unpolarised spectrum is the sum of s and p spectra and the spectra are normalised to the height of the maximum of the unpolarised spectrum. The step barrier height was taken the same for all the cases ($V_0 = 0.94$ Ryd) and the energy zeroes are the muffin-tin zeroes of the potentials used (derived from a self-consistent LMTO calculation).

Looking at figure 4 one can see the effect of increasing the atomic number. The spin–orbit interaction produces a split in the low energy peak, which is very small for Cu (upper panel), about 0.5 eV for Ag (middle panel), and about 1.5 eV for Au (lower panel). These values are related to the splitting of the Γ_8^+ states along the Λ direction, and show how a relativistic theory is necessary to understand the details of the electronic states of a metal. The agreement of the spectra in figure 4 with the experimental data of Courths *et al* (1984) is remarkable. The overall shapes of the features are in sensible agreement, but the relative heights of the peaks are slightly different. The relative positions of the peaks are correct within few tenths of an eV, and the surface states are found at the right energies, if a little distorted in shape. The computer code for calculating these spectra is a generalisation of the available non-relativistic code (Hopkinson *et al* 1980), and for the calculations shown it took few seconds of CRAY-XMP/48 machine per

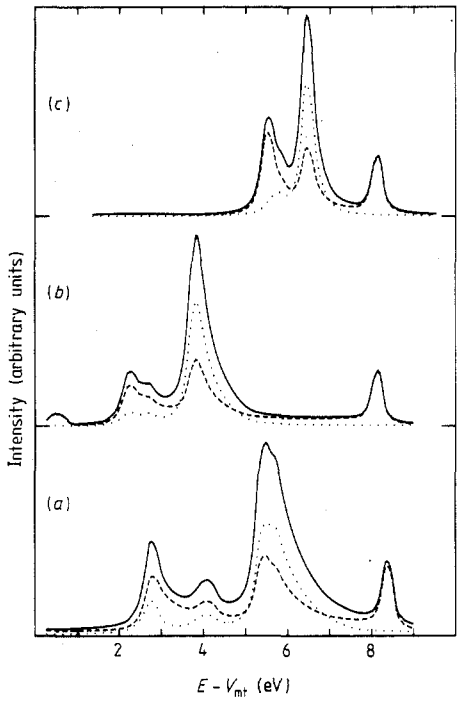

Figure 4. The calculated photoemission spectra from the (1, 1, 1) surface of Au (*a*), Ag (*b*), and Cu (*c*). Unpolarised spectra: full curves; s-polarised spectra: dotted curves; p-polarised spectra: broken curves. $\hbar\omega = 21.2$ eV; $(\theta_p, \varphi_p) = (50, 0)$; $(\theta_e, \varphi_e) = (\pi, 0)$.

energy point, being about a factor of six slower than the corresponding non-relativistic calculation.

Another very interesting point concerns the spin structure of the photocurrent. It is now well established that circularly polarised light extracts spin-polarised photoelectron beams (Fano 1969), as experiments and calculations have shown for the case of Pt (1, 1, 1) surface (Eyers *et al* 1984, Ginatempo *et al* 1985, Ackermann and Feder 1985). Moreover Tamura *et al* (1987) have shown on the basis of symmetry arguments and analytical and numerical calculations, that it is also possible to extract spin-polarised photoelectrons using linearly polarised radiation. This interesting effect happens in the case of (1, 1, 1) surfaces of FCC lattices, because there is no mirror plane perpendicular to a given mirror plane, orthogonal to the surface itself. Due to this fact the electron spin-polarisation vector $\boldsymbol{P}$ has a component parallel to the surface. We performed the calculation of the spin-polarisation, as indicated in § 2.2, for the case of the (1, 1, 1) surface of Au using linearly polarised radiation, and the results confirm Tamura *et al*'s (1987) statement.

3. The random alloy case

The multiple-scattering treatment used in the former section allows for an extension to the case of random alloys, following the procedure used by Durham (1981). As we mentioned before, there is a direct link between band structure of a pure metal and the angle-resolved photoemission spectra. For a random alloy the same link is between the Bloch spectral functions, the 'alloy band structure', and the ARPES.

For a random alloy containing heavy elements the only available first-principles method is the relation KKR–CPA of Staunton *et al* (1980). It is based on the coherent potential approximation, which describes the average Green function by the Green function for an electron moving in the field of an ordered array of effective scatterers. These are described by the coherent t-matrix t_c, which is the solution of the following system of equations

$$\begin{cases} \tau_c^{00}(E) = \dfrac{1}{\Omega_{BZ}} \displaystyle\int \mathrm{d}\boldsymbol{k}[t_c^{-1}(E) - G_{KKR}^0(\boldsymbol{k}, E)]^{-1} \\ c[(t_a^{-1} - t_c^{-1})^{-1} + \tau_c^{00}]^{-1} + (1-c)[(t_b^{-1} - t_c^{-1})^{-1} + \tau_c^{00}]^{-1} = 0. \end{cases} \tag{58}$$

The matrices involved in these equations are to be considered in the double point group representation (Onodera and Okazaki 1966). The main difference from pure metals is the nature of the single site coherent t-matrix t_c. In particular, it corresponds to an inelastic scatterer, which has only the full cubic symmetry and is no longer a diagonal matrix. Recently, Ginatempo and Staunton (1988) suggested an efficient and reliable method to solve this system of equations in the double-point-group representation. Among other things their calculation yields the Bloch spectral function (see also Faulkner and Stocks 1980)

$$A_B(k, E) = -\frac{\mathrm{Im}}{\pi} \mathrm{Tr} \left\{ \sum_{\alpha,\beta} c_\alpha c_\beta \tilde{D}_\alpha Z_{\alpha\beta} D_\beta (\tau_c(k, E) - \tau_c^{00}(E)) + \sum_\alpha c_\alpha Z_{\alpha\alpha} D_\alpha \tau_c^{00}(E) \right\} \tag{59}$$

where α, β run over the atomic species, the CPA 'projector' D_α is:

$$D_\alpha = [1 + (t_\alpha^{-1} - t_c^{-1})^{-1} \tau_c^{00}]^{-1} \tag{60}$$

and the 'matrix elements' are:

$$Z_{\alpha\beta}^{\kappa\mu} = \int_{u.c.} \mathrm{d}\boldsymbol{r}\, \psi_{\kappa\mu}^{\alpha\dagger}(\boldsymbol{r}, \varepsilon) \psi_{\kappa\mu}^{\beta}(\boldsymbol{r}, \varepsilon). \tag{61}$$

It is noteworthy that equation (59) has a similar structure to equation (52), but there the coefficients $A_{\kappa\mu}^{\lambda}$ contain information about the multiple scattering of the final time-reversed LEED state.

Now one can average, using CPA, the photocurrent in equations (49)–(55). Following Durham (1981) we find:

$$\langle I^{\lambda\lambda} \rangle = \langle I^{\lambda\lambda} \rangle_{at} + \langle I^{\lambda\lambda} \rangle_{mult} + \langle I^{\lambda\lambda} \rangle_{surf}. \tag{62}$$

The average of the surface term is trivial. For the atomic term we find

$$\langle I^{\lambda\lambda} \rangle_{at} = c\, I_{at}^{a\lambda\lambda} + (1-c)\, I_{at}^{b\lambda\lambda} \tag{63}$$

where the notation is obvious. The multiple scattering term, however requires more attention (angular momentum indices are dropped for sake of clarity):

$$\langle I^{\lambda\lambda} \rangle_{mult} = I_{coh}^{\lambda\lambda} + I_{inc}^{\lambda\lambda} \tag{64}$$

$$I_{coh}^{\lambda\lambda} = -\frac{\mathrm{Im}}{\pi} \sum \{ A^{n\lambda} D^{\dagger} M_c^{n(2)} (\tau_c^n(-k_\parallel + q, E) - t_c) M_c^{n(1)} D A^{n\lambda *} \} \tag{65}$$

$$I_{\text{inc}}^{\lambda\lambda} = -\frac{\text{Im}}{\pi}\sum\{c[A^{n\lambda}D^{\dagger}M_a^{n(2)}(\tau_a^{n00} - t_a)M_a^{n(1)}DA^{n\lambda *}] + (1-c)[A^{n\lambda}D^{\dagger}M_b^{n(2)}(\tau_b^{n00} - t_b)M_b^{n(1)}DA^{n\lambda *}] - [A^{n\lambda}D^{\dagger}M_c^{n(2)}\tau_c^{n00}(\varepsilon)M_c^{n(1)}DA^{n\lambda *}]\} \tag{66}$$

where the effective dipole radial integral is

$$M_{cKK'}^{n(i)} = \sum_{K''\mu''}(c\tilde{D}_{aK\mu K''\mu''}M_{aK''K'}^{n(i)} + (1-c)\tilde{D}_{bK\mu K''\mu''}M_{bK''K'}^{n(i)}]. \tag{67}$$

The 'α-partial' τ matrix (the conditional CPA average fixing the α species in the 0-th site) is

$$\tau_{\alpha}^{00} = D_{\alpha}\cdot\tau_c^{n00} = \tau_c^{n00}\cdot\tilde{D}_{\alpha} \tag{68}$$

and the calculation for the high energy state amplitude $A_{K\mu}^{n\lambda}$ (cf equations (41) and (42)) is performed by means of the averaged t-matrix approximation (ATA) for the high-energy scattering amplitude:

$$t_c^{\text{ATA}}(E+\hbar\omega) = ct_a(E+\hbar\omega) + (1-c)t_b(E+\hbar\omega). \tag{69}$$

Such an approximation is justified by the fact that usually at high energy CPA and ATA tend to coincide. Finally, note that in arriving at equations (65) and (66) we have averaged the product of three τ matrices by making the following approximation:

$$\langle\tau(E+\hbar\omega)\,\tau(E)\,\tau^{\dagger}(E+\hbar\omega)\rangle \cong \tau^{\text{ATA}}(E+\hbar\omega)\,\tau_c(E)\,\tau^{\dagger\text{ATA}}(E+\hbar\omega). \tag{70}$$

This means neglecting even the CPA vertex corrections (Szotek *et al* 1984). According to Durham (1981) to neglect those is consistent with the ATA. The meanings of coherent and incoherent intensities ($I_{\text{coh}}^{\lambda\lambda}$ and $I_{\text{inc}}^{\lambda\lambda}$ respectively) also follow the nomenclature introduced by Durham (1981).

One of the many interesting consequences of the above theory concerns the spin-polarisation. Evidently, in the case of a random alloy, the biggest contribution to P_z should come from those states and k-points where spin–orbit interaction is stronger. Therefore for an alloy made by a light and a heavy element with a split-band behaviour (say Cu–Au or Ni–Pt) a measurement of P_z might help to identify the states related to the heavy element, provided the right final state has been selected. Such a remark is of course applicable to ordered alloys as well.

Another interesting experimental possibility for highlighting the $A(B)$ related bands at the expense of the contributions from the $B(A)$ related bands is suggested by the Cooper minima. Different elements will have such minima in different ranges of photon frequency, therefore with a careful study such a theory might predict where to look for successfully identifying A and B states by means of ARPES.

4. The photoemission spectra of Cu_3Au in the ordered and disordered state

Our first aim in this section is to demonstrate the tractability of the above theory for random alloys by explicit calculations for $Cu_{0.75}Au_{0.25}$. Secondly, we will show results using the many-atom-per-unit-cell version of the theory of § 2 for the ordered intermetallic compound Cu_3Au. By picking these two particular examples to illustrate the uses of the two newly accessible sectors of a fairly general theory of photoemission from metals, we wish to focus attention on a new opportunity created by their combined use for studying the role of the electronic structure in order–disorder transformations.

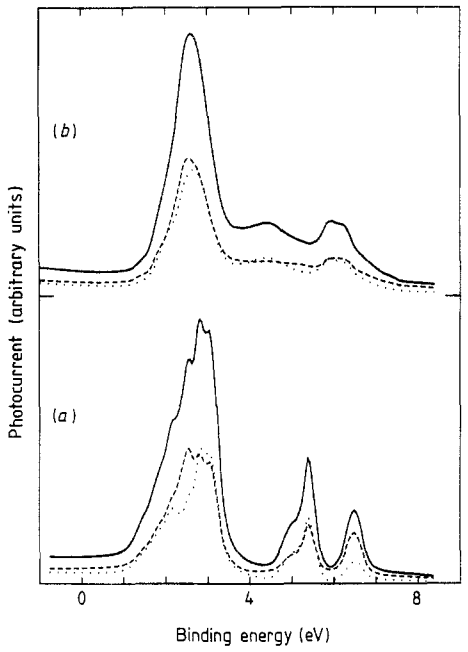

Figure 5. The calculated photoemission spectra from the (1, 0, 0) surface of ordered (*a*) and disordered (*b*) Cu_3Au alloy. Notation for unpolarised, s- and p-polarised spectra as in figure 4. $\hbar\omega$ = 40 eV; $(\Theta_p, \varphi_p) = (30, 0)$; $(\Theta_e, \varphi_e) = (\pi, 0)$.

The question of what drives the famous order–disorder transition of Cu_3Au, from the low temperature $L1_2$ structure at $T = 683$ K to the high temperature FCC solid-solution state, is of seminal interest (Khachaturian 1983). Clearly an attractive suggestion is that, by studying the electronic structure with photoemission below and above the phase transition one may hope to identify its electronic cause. The calculations we shall present in this section will constitute evidence that such hope is justified.

In short, using the theories of §§ 2 and 3, we have studied the normal emission spectra from the (1, 0, 0) surface of Cu_3Au in both the ordered and disordered phases respectively. The incidence angle was chosen to be $\Theta_p = 30°$. We took the plane of emission to be the ΓXWK, and the photon frequency to be $\hbar\omega = 40$ eV, in both cases. The potential functions used in both sets of calculations were the same. They were determined by a self-consistent LMTO calculation (Temmerman 1988). The electronic structure of the solid solution was that determined by the KKR–CPA relation calculations of Ginatempo and Staunton (1988).

Figure 5 shows respectively (*a*) the ordered and (*b*) the disordered spectra for s, p and unpolarised light. The spectra have been normalised to the height of the main peak of corresponding unpolarised spectra. The energy zero in figure 5 corresponds to the Fermi level of the ordered alloy.

Comparing the two panels one can immediately see how the effect of the disorder is the smearing out of the ordered features leaving the main peak at 2.8 eV (arising from Cu related states) and the peak at 6.5 eV (Au related) essentially unchanged, apart from a shift. Much bigger are the changes of the peaks at 4.9 and 5.4 eV, which, particularly for the p-polarised spectra, almost disappear. These are the compound-related states and characterise the Cu_3Au $L1_2$ structure. Evidently, it is tempting to regard these states as the principle carrier of the electronic driving force behind the order–disorder transformation. A full analysis of the experimental data in terms of calculations as the above throws useful light on this suggestion and will be published elsewhere.

5. Conclusion

We have presented a relativistic theory for the angle- and spin-resolved photoemission from ordered and disordered non-magnetic metals, and illustrated its use by explicit calculations on the noble metals and on the Cu_3Au system. We have also presented a transformation of the relativistic dipole matrix element into its relativistic acceleration form and discussed useful new features of the new formula. It was argued that the flexibility of this theory enables us to calculate the ARPES spectra of ordered and disordered alloy on an equal footing, and that such calculations can help to clarify the role of the electronic structure in the order–disorder transformations. A detailed comparison between theoretical and experimental data on Cu_3Au will be published in a separate paper.

Acknowledgments

We would like to acknowledge the contribution by encouragement and enlightening discussions of Drs Robin G Jordan and Julie B Staunton. One of use (BG) wishes to acknowledge the Consiglio Nazionale delle Ricerche (Italy) for supporting CRAY–XMP resources at CINECA (Bologna) where the codes for the ordered and disordered alloy have been developed.

References

Ackermann B and Feder R 1985a *J. Phys. C: Solid State Phys.* **18** 1093
—— 1985b *Sol. State Com.* **54** 1077
Caroli C, Lederer-Rozenblatt D, Roulet B and Saint-James D 1973 *Phys. Rev.* B **8** 4552
Christensen N E and Christensen O B 1986 *Phys. Rev.* B **33** 4739
Cooper J W 1962 *Phys. Rev.* **128** 681
Courths R, Wern H, Hau U, Cord B, Bachelier V and Hüfner S 1984 *J. Phys. F: Met. Phys.* **14** 1559
Durham P J 1981 *J. Phys. F: Met. Phys.* **11** 2475
Durham P J, Temmerman W M, Larsson C G and Nilsson P O 1983 *Vacuum* **33** 771
Eckardt H, Fritsche L and Noffke J 1984 *J. Phys. F: Met. Phys.* **14** 97
Eyers A, Shafers A, Schonhense G, Heinzmann U, Oepen H P, Hunlich K, Kirschner J and Borstel G 1984 *Phys. Rev. Lett.* **52** 1559
Fano U 1969 *Phys. Rev.* **178** 131
Fano U and Cooper J W 1968 *Rev. Mod. Phys.* **40** 441
Fasol G, Christensen N E and Cardona M 1988 *Phys. Rev.* B **38** 1806
Faulkner J S 1982 *Progr. Mater. Sci.* **27** 3
Faulkner J S and Stocks G M 1980 *Phys. Rev.* B **21** 3222
Feder R 1981 *J. Phys. C: Solid State Phys.* **14** 2049
Feder R 1985 *Polarised Electrons in Surface Physics* ed. R Feder (Singapore: World Publishing)
Ginatempo B, Durham P J, Gyorffy B L and Temmerman W M 1985 *Phys. Rev. Lett.* **54** 1581
Ginatempo B and Staunton J B 1988 *J. Phys. F: Met. Phys.* **18** 1827
Gyorffy B L, Johnson D D, Pinski F J, Nicholson D M and Stocks G M 1988 in *Alloy Phase Stability* ed. A Gonis and G M Stocks (NATO-ASI series) to be published
Himpsel F J 1983 *Adv. Phys.* **32** 1
Hopkinson J F L, Pendry J B and Titterington D J 1980 *Comp. Phys. Commun.* **19** 69
Jordan R G and Durham P J 1988 *Alloy Phase Stability* ed. G M Stocks and A Gonis (NATO-ASI series) to be published
Jordan R G, Sohal G S, Gyorffy B L, Durham P J, Temmerman W M and Weinberger P 1985 *J. Phys. F: Met. Phys.* **15** L135
Khachaturian A G 1983 *Theory of Structural Transformations in Solids* (New York: Wiley)

Kim Y S, Ron A, Pratt R H, Tambe P R and Manson S T 1981 *Phys. Rev. Lett.* **46** 1326
Knapp J A, Himpsel F J and Eastmann D E 1979 *Phys. Rev.* B **19** 4952
Mahan G D 1970 *Phys. Rev.* B **2** 4334
McDonald A H, Daams J M, Vosko S H and Koelling D D 1981 *Phys. Rev.* B **23** 6377
McDonald A H and Vosko S H 1979 *J. Phys. C: Solid State Phys.* **12** 2977
Onodera Y and Okazaki M 1966 *J. Phys. Soc. Japan* **21** 2400
Pendry J B 1974 *Low Energy Electron Diffraction* (London: Academic)
Pendry J B 1976 *Surf. Sci.* **57** 679
Rajagopal A K 1978 *J. Phys. C: Solid State Phys.* **11** L943
Rose M E 1961 *Relativistic Electron Theory* (New York: Wiley)
Schaich W L and Ashcroft N W 1971 *Phys. Rev.* B **3** 2452
Staunton J B, Gyorffy B L and Weinberger P 1980 *J. Phys. F: Met. Phys.* **10** 2665
Staunton J B, Weinberger P and Gyorffy B L 1983 *J. Phys. F: Met. Phys.* **13** 779
Stocks G M and Winter H 1985 *The Electronic Structure of Complex Systems* ed. P Phariseau and W M Temmerman (New York: Plenum)
Szotek D, Gyorffy B L, Stocks G M and Temmerman W M 1984 *J. Phys. F: Met. Phys.* **14** 2571
Tamura E, Piepke W and Feder R 1987 *Phys. Rev. Lett.* **59** 934
Temmerman W M 1988 private communication
Temmerman W M, Durham P J, Szotek Z, Sob M and Larsson C G 1988 *J. Phys. F.: Met. Phys.* **18** 2387
Williams R H, Srivastava G P and McGovern I T 1980 *Rep. Prog. Phys.* **43** 1357